Electronic Supplementary Material (ESI) for Nanoscale.

Supporting Information

Er^{3+}-to-Yb^{3+} and Pr^{3+}-to-Yb^{3+} energy transfer for highly efficient near-infrared cryogenic optical temperature sensing

Anna M. Kaczmarek,[a]* Mariusz K. Kaczmarek,[b] Rik Van Deun[a]*

Experimental Section

Synthesis of Ln^{3+} doped LaF_3 nanoparticles

Chemicals: All chemicals were bought from Sigma Aldrich or VWR and were used without further purification.

The synthesis was based on that reported by Shan et al and only slightly modified.[1] 2.0 g of D-glucose was dissolved in 20 mL distilled water. To this 0.156 g NaF was added while stirring and was heated up to 60 °C. Appropriate amounts of the different $Ln(NO_3)_3 \cdot 6H_2O$ (in total 0.152 mmol) were dissolved in 4 mL distilled water and added to the D-glucose and NaF solution. The reaction was left to stir for 24 h. Afterwards it was switched off and cooled down to room temperature. The nanoparticles were precipitated out of the solution by raising the pH to 9-10 using 1 M NaOH. The precipitate was collected through centrifugation and washed three times with water before drying in a vacuum oven at 60 °C. Last the powders were heat treated at 600 °C in a furnace oven for 3h to enhance luminescence properties.

Characterization

Powder X-Ray diffraction (XRD) patterns were measured on a Thermo Scientific ARL X'TRA diffractometer equipped with a Cu Ka (l = 1.5405 Å) source, a goniometer and a Peltier cooled Si(Li) solid state detector. X-ray fluorescence (XRF) was measured by XRF Supermini200 Rigaku to analyse the relative Ln^{3+} contents. Transmission Electron Microscopy (TEM) images were carried out by using a Cs-corrected JEOL JEM2200FS transmission electron microscope with the working voltage of 200 kV. The photoluminescence spectra were recorded on an Edinburgh Instruments FLSP 920 UV-vis-NIR spectrofluorimeter with a 450 W xenon lamp as the steady state excitation source. A Hamamatsu R928P photomultiplier tube was used to detect the emission signals in the near-UV to visible range. A Hamamatsu R5509–72 photomultiplier was used to detect emission in the NIR region. The temperature-dependent measurements were performed using an ARS closed cycle cryostat. All temperature-dependent calculations were performed employing the TeSen software (http://www.tesen.ugent.be).

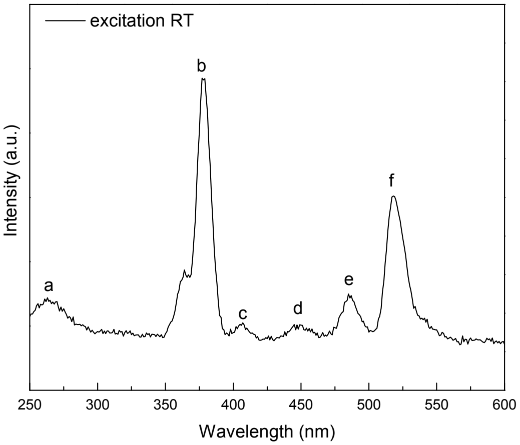

Figure S1 Excitation spectrum of 2.96%Er^{3+},1.57%Yb^{3+}: LaF_3 recorded at room temperature (observed at 988.3 nm).

Table S1 Assignment of peaks for 2.96%Er^{3+},1.57%Yb^{3+}: LaF_3 recorded at room temperature (Figure S1)

Label	Wavelength (nm)	Wavenumber (cm^{-1})	Transitions
a	263.9	37893	$^2D_{5/2}\leftarrow{}^4I_{15/2}$
b	377.9	26462	$^4G_{11/2}\leftarrow{}^4I_{15/2}$
c	406.7	24588	$^2G_{9/2}$, $^4F_{9/2}\leftarrow{}^4I_{15/2}$
d	446.5	22396	$^4F_{3/2}$, $^4F_{5/2}\leftarrow{}^4I_{15/2}$
e	485.8	20584	$^4F_{7/2}\leftarrow{}^4I_{15/2}$
f	518.9	19271	$^4H_{11/2}\leftarrow{}^4I_{15/2}$

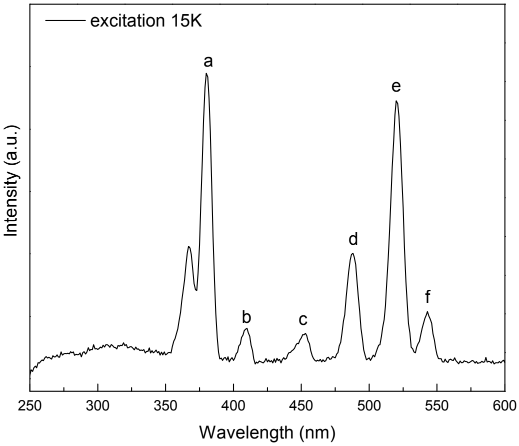

Figure S2 Excitation spectrum of 2.96%Er^{3+},1.57%Yb^{3+}: LaF_3 recorded at 15 K (observed at 988.3 nm).

Table S2 Assignment of peaks for 2.96%Er^{3+},1.57%Yb^{3+}: LaF_3 recorded at 15 K (Figure S2)

Label	Wavelength (nm)	Wavenumber (cm^{-1})	Transitions
a	380.2	26302	$^4G_{11/2}\leftarrow{}^4I_{15/2}$
b	408.8	24462	$^2G_{9/2}$, $^4F_{9/2}\leftarrow{}^4I_{15/2}$
c	451.5	22148	$^4F_{3/2}$, $^4F_{5/2}\leftarrow{}^4I_{15/2}$
d	487.5	20534	$^4F_{7/2}\leftarrow{}^4I_{15/2}$
e	519.7	19268	$^4H_{11/2}\leftarrow{}^4I_{15/2}$
f	543.5	18399	$^4S_{3/2}\leftarrow{}^4I_{15/2}$

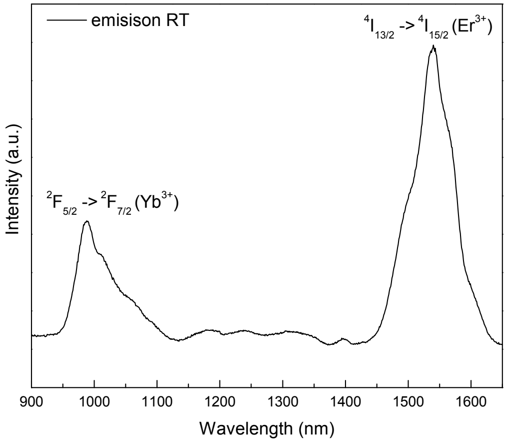

Figure S3 Emission spectrum of 2.96%Er^{3+},1.57%Yb^{3+}: LaF$_3$ recorded at room temperature (excited at 377.9 nm and observed at 1539.8 nm).

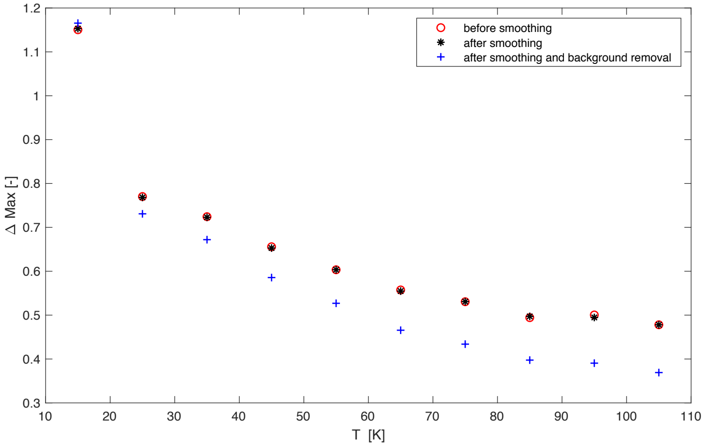

Figure S4 Effect of data pre-processing on Δ calculated based on peak maxima (5 point S-G smoothing and background removal have been applied) for 2.96%Er^{3+},1.57%Yb^{3+}: LaF$_3$.

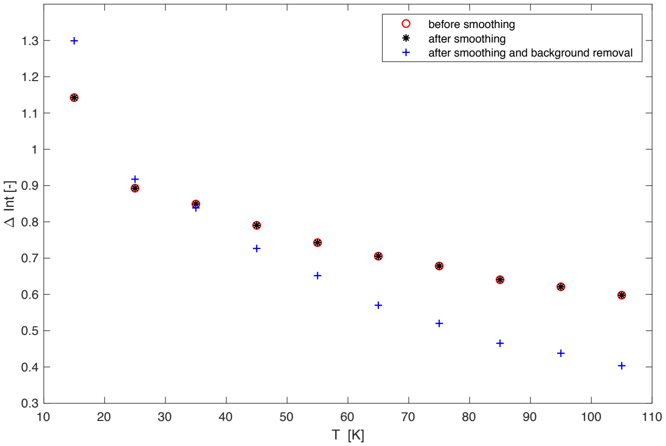

Figure S5 Effect of data pre-processing on Δ calculated based on integrated areas under peaks (5 point S-G smoothing and background removal have been applied) for 2.96%Er^{3+},1.57%Yb^{3+}: LaF_3.

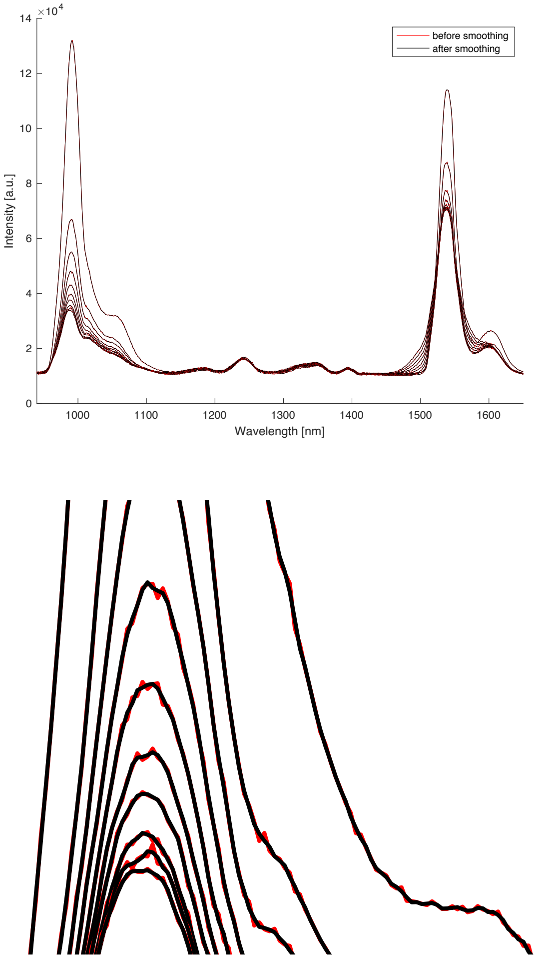

Figure S6 Top: emission spectra measured in the 15 – 105K temperature range before and after smoothing for 2.96%Er^{3+},1.57%Yb^{3+}: LaF_3. Bottom: zoom in on the emission spectra for better visibility of emission curve smoothing.

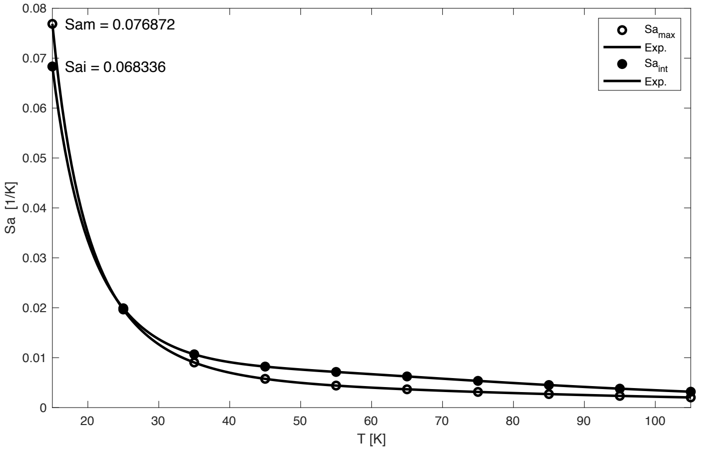

Figure S7 Plot presenting the absolute sensitivity Sa values at varied temperatures (15 – 105K) for 2.96%Er^{3+},1.57%Yb^{3+}: LaF_3. The opened points show results for the peak maxima, whereas the filled points show results for the integrated areas under the peaks. The solid lines are guides for the eye.

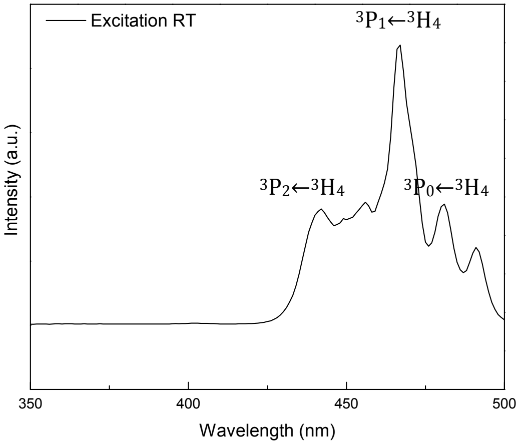

Figure S8 Excitation spectrum of 2.20%Pr^{3+},1.45%Yb^{3+}: LaF_3 recorded at room temperature (observed at 978.1 nm).

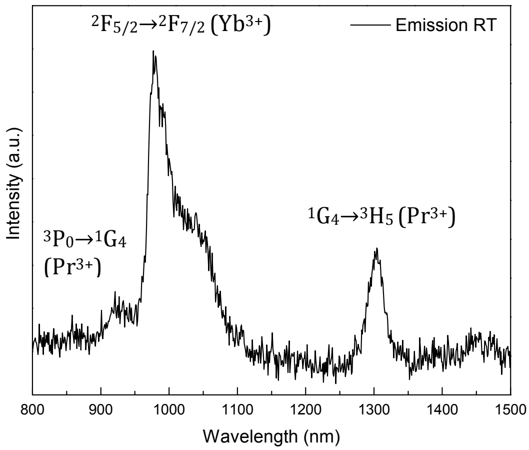

Figure S9 Emission spectrum of 2.20%Pr^{3+},1.45%Yb^{3+}: LaF$_3$ recorded at room temperature (excited at 467.0 nm, observed at 978.1 nm). The emission spectrum was not smoothed.

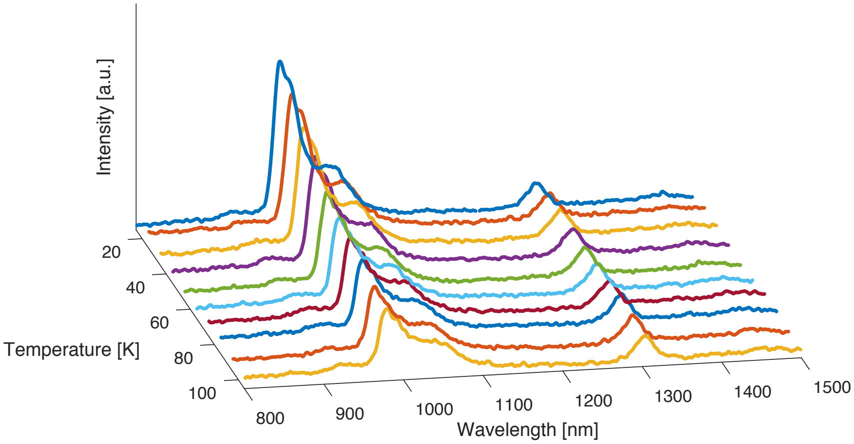

Figure S10 Emission map of 2.20%Pr^{3+},1.45%Yb^{3+}: LaF$_3$ recorded in the 15 – 105K temperature range. The data was smoothed employing 5 point S-G smoothing.

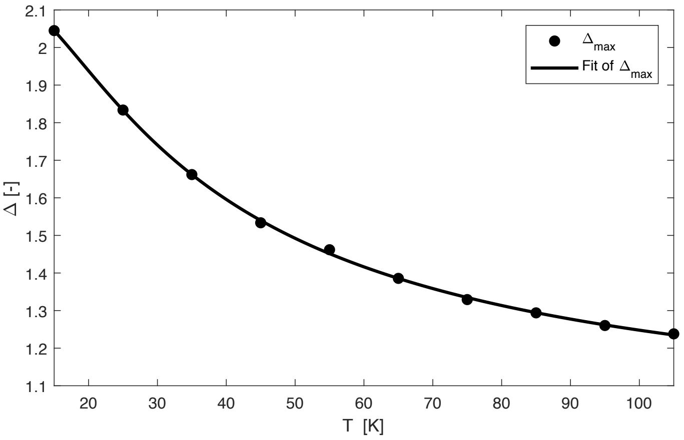

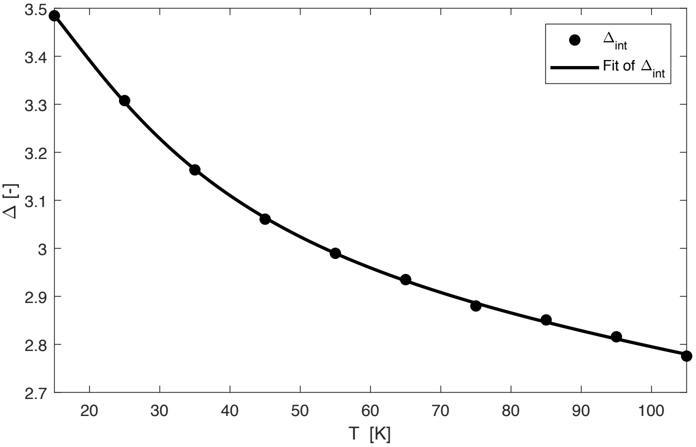

Figure S11 Plots presenting the calibration curves for compound 2.20%Pr^{3+},1.45%Yb^{3+}: LaF_3 when equation 4 is employed. The points show the experimental Δ parameters and the solid lines show the best fit of the experimental points using equation 4. Top: the graph represents Δ calculated from the peak maxima; bottom: the graph represents the Δ calculated from the integrated areas under the peaks.

Based on the peak maxima as well as the integrated areas under the peak the experimental thermometric parameters were determined ($I_{978.1}/I_{1302.5}$) for the 2.20%Pr^{3+},1.45%Yb^{3+}: LaF_3 sample. They could be well fitted employing equation 4 yielding R^2 = 0.99971 (for peak maxima) and R^2 = 0.99975 (for integrated area under the peaks). For calculations based on peak maxima the equation fit yielded

Δ_0= 2.15, $\alpha 1$ =0.18, $\Delta E1$ = 87.02 cm^{-1}, $\alpha 2$ =1.05, $\Delta E2$ = 31.54 cm^{-1}. For calculations based on integrated areas under the peaks the equation fit yielded Δ_0= 3.59, $\alpha 1$ =0.63, $\Delta E1$ = 286.13 cm^{-1}, $\alpha 2$ =0.40, $\Delta E2$ = 26.32 cm^{-1}. The larger non-radiative deactivation energy ($\Delta E1$) probably involves the $^1G_4$ level of Pr^{3+} and the $^2F_{5/2}$ level of Yb^{3+}. The smaller non-radiative deactivation energy ($\Delta E2$) most likely involves non-radiative deactivation through the multiple Pr^{3+} local sites (Pr^{3+}-Pr^{3+} energy migration). The maximum value of S_a was 0.020131K^{-1} (at 15K) for peak maxima, and 0.018408K^{-1} (at 15K) for integrated areas under the peaks. The maximum S_r value was 1.0839 %K^{-1} (at 25K) for peak maxima, and 0.52814%K^{-1} (at 15K) for integrated areas under the peaks. The S_r plot calculated for both peak maxima and integrated areas under the peaks has been presented in Figure S12.

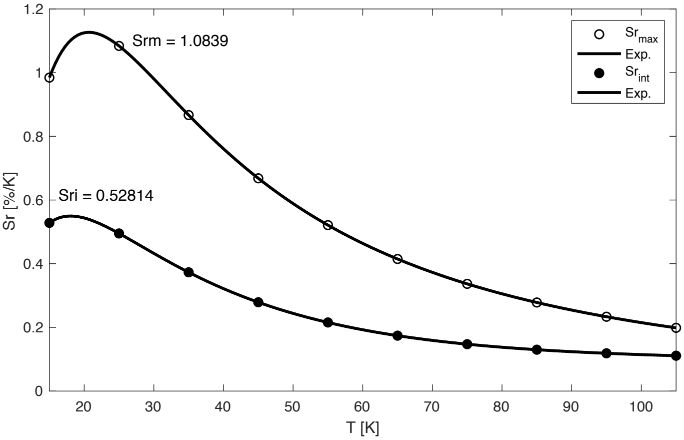

Figure S12 Plot presenting the relative sensitivity S_r values at varied temperatures (15 – 105K) for 2.20%Pr^{3+},1.45%Yb^{3+}: LaF$_3$. The opened points show results for the peak maxima, whereas the filled points show results for the integrated areas under the peaks. The solid line is a guide for the eye.

The two samples discussed in the manuscript (2.96%Er^{3+},1.57%Yb^{3+}: LaF$_3$ and 2.20%Pr^{3+},1.45%Yb^{3+}: LaF$_3$) were not prepared through trail-and -error approach in an attempt to obtain best temperature-dependent luminescence properties, but were designed based on our own knowledge and available literature. For example in the case of the Er/Yb material we aimed for a material, which would show a strong emission signal of Yb^{3+} (as it decreases in intensity with temperature increase) and a low intensity peak of Er^{3+} (yet being still well detectable from the background). At the same time we considered potential concentration quenching of the Ln^{3+} ions and the cost of producing our material (aiming at low doping percentages of the Ln^{3+} ions, which still give sufficiently strong signal). This resulted in a 3% : 1.5% Er : Yb ratio employed for these materials. To confirm the correctness of our approach we have synthesized three additional Er/Yb and three additional Pr/Yb samples and analysed their (temperature-dependent) luminescence properties.

Below Table S3 overviews the chosen molar doping ratios and real lanthanide contents (based on XRF are presented). The temperature-dependent properties of 2.84%Er, 1.12%Yb: LaF$_3$, 3.24%Er, 4.09%Yb:LaF$_3$, and 3.01%Er, 4.72%Yb:LaF$_3$ are presented below. For the Pr/Yb samples we observed that a higher doping percentages than 2.20%Pr, 1.45%Yb in the LaF$_3$ matrix resulted in concentration quenching. Similar observations have been reported in literature.[2] Employing lower doping percentages than 2.20%Pr, 1.45%Yb was not optimal due to the low signal of these samples in the cryostat when measuring in the NIR region.

Table S3. Relative Ln^{3+} contents for the x%Ln: LaF$_3$ samples during synthesis (calcd.) and as determined by XRF.

Sample	Molar amounts used in synthesis [mmol]			La^{3+} ion		Er^{3+}/Pr^{3+} ion		Yb^{3+} ion	
	La(NO$_3$)$_3$	Er(NO$_3$)$_3$/ Pr(NO$_3$)$_3$	Yb(NO$_3$)$_3$	Calcd.	XRF	Calcd.	XRF	Calcd.	XRF
3%Er, 1%Yb:LaF3	0.96	0.03	0.01	96%	95.96%	3%	2.84%	1%	1.12%
3%Er, 1.5%Yb:LaF$_3$	0.955	0.03	0.015	95.5%	95.47%	3%	2.96%	1.5%	1.57%
3%Er, 3%Yb:LaF$_3$	0.94	0.03	0.03	94%	92.67%	3%	3.24%	3%	4.09%
3%Er, 5%Yb:LaF$_3$	0.92	0.03	0.05	92%	92.18%	3%	3.01%	5%	4.72%
3%Pr, 1.5%Yb:LaF3	0.955	0.03	0.015	95.5%	96.35%	3%	2.20%	1.5%	1.45%
3%Pr, 3%Yb:LaF3	0.94	0.03	0.03	94%	93.83%	3%	3.06%	3%	3.11%
3%Pr, 5%Yb:LaF3	0.92	0.03	0.05	92%	92.11%	3%	3.02%	5%	4.87%
3%Pr, 10%Yb:LaF3	0.87	0.03	0.10	90%	85.35%	3%	2.33%	10%	12.32%

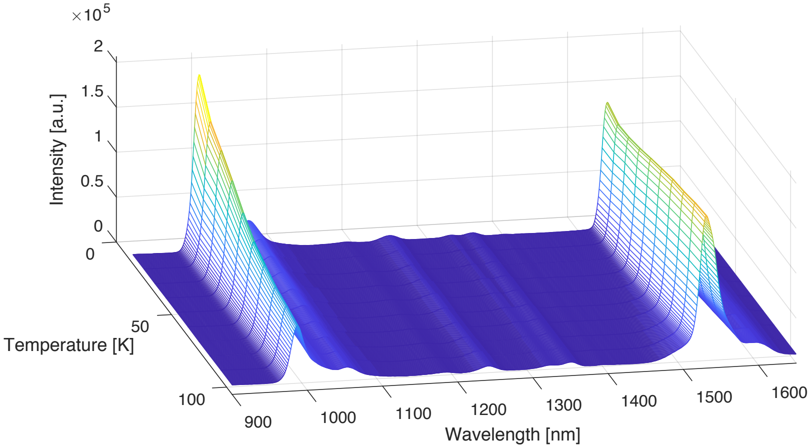

Figure S13 Emission map of 2.84%Er^{3+},1.12%Yb^{3+}: LaF_3 recorded in the 15 – 105K temperature range. The data was smoothed employing 5 point S-G smoothing.

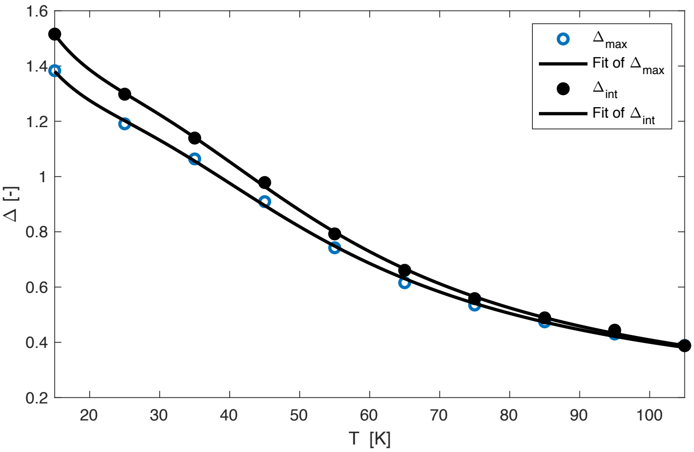

Figure S14 Plot presenting the calibration curves for compound 2.84%Er^{3+},1.12%Yb^{3+}: LaF_3 when equation 4 is employed. The points show the experimental Δ parameters and the solid lines show the best fit of the experimental points using equation 4. The opened points represent Δ calculated from the peak maxima, whereas the filled points represent the Δ calculated from the integrated areas under the peaks. (R^2 = 0.99244 for peak maxima and R^2 = 0.99127 for integrated area under the peaks)

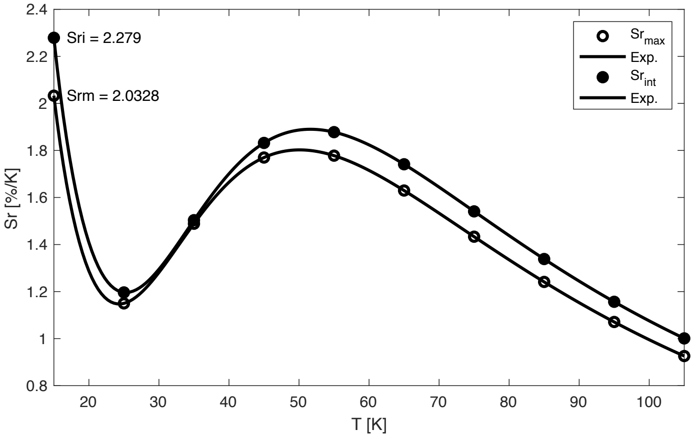

Figure S15 Plot presenting the relative sensitivity Sr values at varied temperatures (15 – 105K) for 2.84%Er^{3+},1.12%Yb^{3+}: LaF_3. The opened points show results for the peak maxima, whereas the filled points show results for the integrated areas under the peaks. The solid lines are guides for the eye.

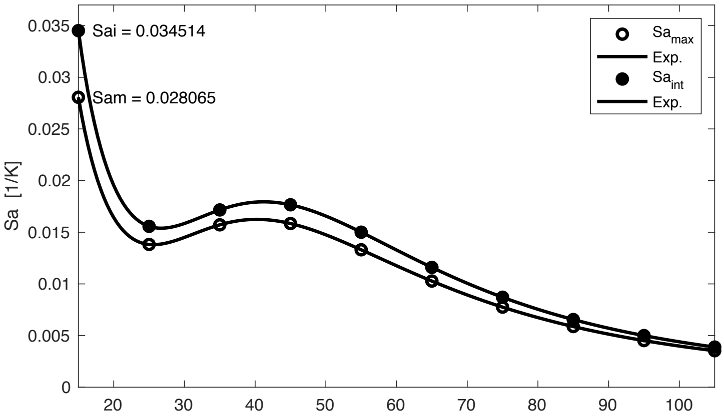

Figure S16 Plot presenting the absolute sensitivity Sa values at varied temperatures (15 – 105K) for 2.84%Er^{3+},1.12%Yb^{3+}: LaF_3. The opened points show results for the peak maxima, whereas the filled points show results for the integrated areas under the peaks. The solid lines are guides for the eye.

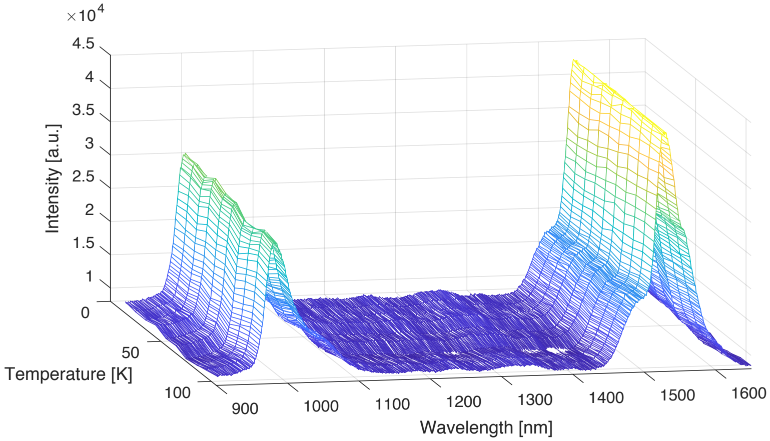

Figure S17 Emission map of 3.24%Er^{3+},4.09%Yb^{3+}: LaF$_3$ recorded in the 15 – 105K temperature range. The data was smoothed employing 5 point S-G smoothing. This sample did not show behavior as a ratiometric temperature sensor in the cryogenic region.

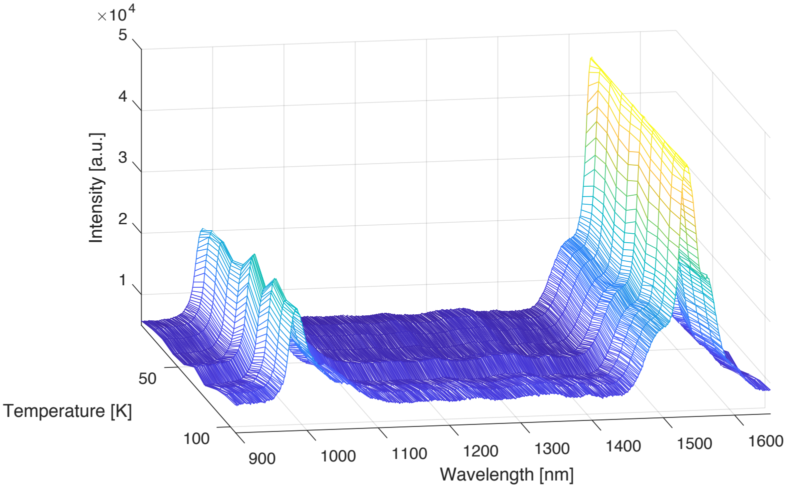

Figure S18 Emission map of 3.01%Er^{3+},4.72%Yb^{3+}: LaF$_3$ recorded in the 15 – 105K temperature range. The data was smoothed employing 5 point S-G smoothing. This sample did not show behavior as a ratiometric temperature sensor in the cryogenic region.

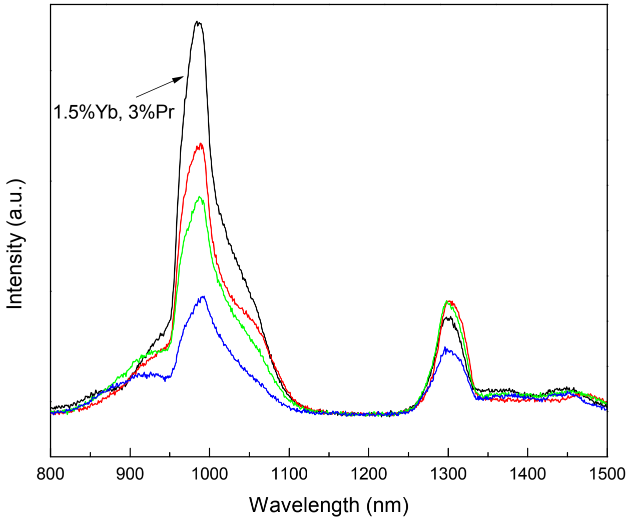

Figure S19 Emission spectra of 2.20%Pr, 1.45%Yb: LaF_3 (black line), 3.06%Pr, 3.11%Yb: LaF_3 (red line), 3.02%Pr, 4.87%Yb: LaF_3 (green line), and 2.33%Pr, 12.32%Yb: LaF_3 (blue line). All samples were excited at 467.0 nm and observed at 978.1 nm.

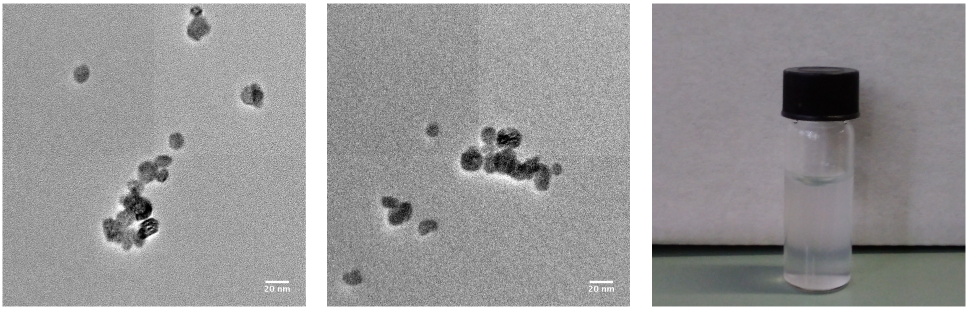

Figure S20 TEM images (left and center) and a photo of a colloidal suspension (right) of 2.96%Er^{3+},1.57%Yb^{3+}: LaF_3 nanoparticles after heat treatment after treated with ultrasound irradiation for 20 – 30 minutes.

[1] G. Shan, M. P. Andrews, T. Gonzalez, H. Djeghelian, Mater. Lett., 2008, 62, 4187-4190.

[2] K. Deng, X. Wei, X. Wang, Y. Chen, M. Yin, Appl. Phys. B, 2011, 102, 555-558.